An Analytical Molecular Mechanics Model for Elastic Properties of Graphyne-*n*

Juan Hou
Shanghai Key Laboratory of Mechanics
in Energy Engineering,
Shanghai Institute of Applied Mathematics and Mechanics,
Shanghai University,
Shanghai 200072, China

Zhengnan Yin
Shanghai Key Laboratory of Mechanics
in Energy Engineering,
Shanghai Institute of Applied Mathematics and Mechanics,
Shanghai University,
Shanghai 200072, China

Yingyan Zhang
School of Computing, Engineering and Mathematics,
University of Western Sydney, Penrith South DC,
New South Wales 2751, Australia

Tienchong Chang[1]
Shanghai Key Laboratory of Mechanics
in Energy Engineering,
Shanghai Institute of Applied Mathematics and Mechanics,
Shanghai University,
Shanghai 200072, China;
State Key Laboratory of Ocean Engineering,
School of Naval Architecture,
Ocean and Civil Engineering,
Shanghai Jiao Tong University,
Shanghai 200240, China
e-mail: tchang@staff.shu.edu.cn

*Graphynes, a new family of carbon allotropes, exhibit superior mechanical properties depending on their atomic structures and have been proposed as a promising building materials for nanodevices. Accurate modeling and clearer understanding of their mechanical properties are essential to the future applications of graphynes. In this paper, an analytical molecular mechanics model is proposed for relating the elastic properties of graphynes to their atomic structures directly. The closed-form expressions for the in-plane stiffness and Poisson's ratio of graphyne-n are obtained for small strains. It is shown that the in-plane stiffness is a decreasing function whereas Poisson's ratio is an increasing function of the number of acetylenic linkages between two adjacent hexagons in graphyne-*n. *The present analytical results enable direct linkages between mechanical properties and lattice structures of graphynes; thereby, providing useful guidelines in designing graphyne configurations to suit their potential applications. Based on an effective bond density analysis, a scaling law is also established for the in-plane stiffness of graphyne-*n *which may have implications for their other mechanical properties.* [DOI: 10.1115/1.4030502]

[1]Corresponding author.
Contributed by the Applied Mechanics Division of ASME for publication in the JOURNAL OF APPLIED MECHANICS. Manuscript received March 9, 2015; final manuscript received April 26, 2015; published online June 16, 2015. Editor: Yonggang Huang.

1 Introduction

From fullerenes, carbon nanotubes to graphene, synthetic carbon allotropes represent a growing fascinating and esthetically pleasing architecture with outstanding materials properties [1], which has attracted a considerable attention to the search for more carbon allotropes [2–4]. Graphynes, a theorized carbon allotrope, are one-atom-thick two-dimensional materials similar to graphene. However, unlike graphene, which has aromatic bonds, graphynes have single and triple bonds. These single and triple bonds lead to potentially unlimited lattice structures, endowing graphynes with versatile mechanical [5–14], electrical [12–21], and chemical properties [22,23]. Therefore, graphynes are more attractive for potential nanoelectromechanical systems (NEMS) applications.

The lattice structure of graphynes can be simply viewed as replacing a portion of the aromatic C–C bonds in graphene by acetylenic linkages with single and triple bonds [3,4]. Different portion of replacements results in different types of graphynes [2–4,17,18]. For example, complete replacement of aromatic bonds by acetylenic linkages in graphene leads to α-graphyne or supergraphene; replacements of two-third, one-third, and fifth-twelfth of aromatic bonds by acetylenic linkages give rise to *β*-, *γ*-, and 6,6,12-graphynes, respectively [2–4]. Furthermore, unlimited graphyne structures are possible by increasing the length of acetylenic chains [2–4,17,18].

Among these different types of graphynes, graphyne-*n*, in which two adjacent benzene hexagons are interconnected by *n* acetylenic linkages (i.e., one-third of aromatic bonds in graphene is replaced by acetylenic linkages, see Fig. 1(*a*)), is of particular interest because of their interesting electronic properties [13,17,19]. As a sister material of graphene, graphynes are expected to possess comparable mechanical properties to graphene. However, numerical results from both molecular dynamics (MD) simulations [6–9] and first-principle calculations [10–13] showed that the in-plane stiffness of graphyne-*n* is substantially lower than that of graphene. Some other mechanical properties, such as Poisson's ratio and shear modulus, are hitherto rarely explored. A clearer and more comprehensive understanding of the mechanical properties of graphynes is needed for their possible applications in NEMS.

In the present work, we use a stick-spiral model to investigate the elastic properties of graphyne-*n*. The stick-spiral model was pioneered by Chang and coworkers [24–27], for analytically linking the elastic properties of carbon nanotubes with their geometric parameters. The model has been also used to study the chirality- and curvature-dependent bending stiffness of graphene [28]. Herein, we extend this model to capture the degradation of the in-plane stiffness of graphyne-*n* with increasing acetylenic linkages.

2 Analytical Model and Results

In the stick-spiral model, the total potential energy, E_t, of carbon allotropes (e.g., carbon nanotubes and graphene) at small strains can be expressed as a sum of energies associated with the variance of bond length (modeled as an elastic stick with an axial stiffness of K_ρ and an infinite bending stiffness), U_ρ, and bond angle (modeled as a spiral spring with a stiffness of C_θ), U_θ [10,19,20].

$$E_t = U_\rho + U_\theta = \sum_i \frac{1}{2} K_\rho (dr_i)^2 + \sum_j \frac{1}{2} C_\theta (d\theta_j)^2 \tag{1}$$

where dr_i is the elongation of bond (stick) i and $d\theta_j$ is the change of bond angle (spiral spring) j.

The main difference in the structure of graphynes from graphene is the presence of the acetylenic chains with repeating single and triple bonds. These acetylenic chains are considered as a carbon allotrope on their own—carbyne [29–32]. According to the previous studies [29–31], the axial stiffness of acetylenic chains can be expressed as

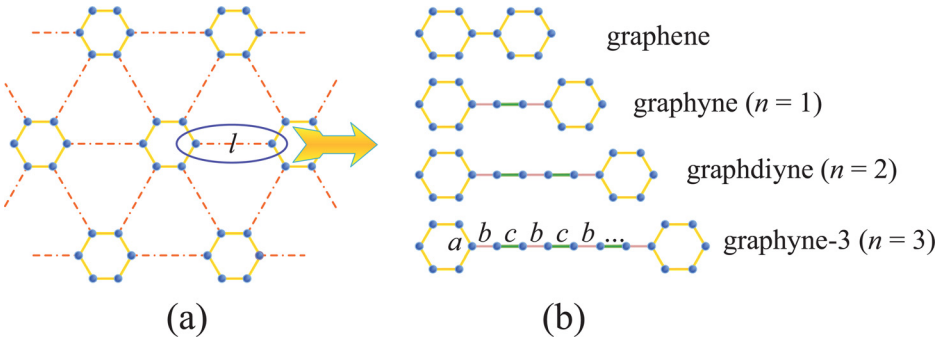

Fig. 1 Schematic illustration of geometric structure (*a*) and bond types (*b*) of graphyne-*n*. Benzene rings with aromatic bonds (labeled *a*) are connected by acetylenic linkages (*l*) with repeating single (*b*) and triple (*c*) bonds.

$$K_n = \frac{Y_{1D}}{l} = \frac{Y_{1D}}{(n+1)b + nc} \tag{2}$$

where Y_{1D} is the one-dimensional tensile modulus (for example, $Y_{1D} = YA$, the product of Young's modulus Y and the cross-sectional area A for beam elements) of carbyne, n is the number of acetylenic linkages, l is the length of acetylenic chains, and b and c are the lengths of single and triple bonds, respectively (Fig. 2(*a*)). The spiral stiffness associated with the bond angle variance in acetylenic chains, C_{bc}, can be related to the bending stiffness of carbyne D as $C_{bc} = 2D/(b+c)$.

When the structure of graphyne-*n* is treated as a stick-spiral system, the elastic properties of graphyne-*n* can be obtained by analyzing the force-deformation response of their unit cells. We consider the case of graphyne-*n* subject to tension along the armchair direction as shown in Fig. 2(*a*). By analyzing the force equilibrium of local structures (Fig. 2(*b*)) in a unit cell, we have the following governing equations:

$$2f_2 = K_n[(n+1)db_a + ndc_a] = K_n dl_a \tag{3}$$

$$\frac{a_z}{2} f_2 \sin\alpha + m_2 = (C_{ab} + 2C_{aa})d\alpha = (C_{ab} + C_{aa})d\alpha + C_{ab}d\beta \tag{4}$$

$$f_2 \cos\alpha = -K_a da_z \tag{5}$$

and

$$f_1 = K_a da_a \tag{6}$$

$$(f_1 - f_2)\cos\beta = -K_n[(n+1)db_z + ndc_z] = -K_n dl_z \tag{7}$$

$$\left(\frac{b_z}{2} + \frac{n}{2}(b_z + c_z)\right)(f_1 - f_2)\sin\beta = C_{ab}(d\alpha + 2d\beta) \tag{8}$$

$$\left((1-(-1)^i)\frac{c_z}{4} + (1+(-1)^i)\frac{b_z}{4} + (n-i)\left(\frac{b_z}{2} + \frac{c_z}{2}\right)\right)(f_1 - f_2)\sin\beta$$

$$= C_{bc}d\phi_i, \quad 1 \le i \le n \tag{9}$$

In the above equations, K_a is the stick stiffness of aromatic bond a (the subscripts a and z represent the bond orientations as shown in Fig. 2(*a*)), C_{aa}, C_{ab}, and C_{bc} are the spiral stiffness of bond angle α, β, and ϕ_i, and f_1, f_2 and m_2 are the internal forces and moment (shown in Fig. 2(*b*)). Based on Eqs. (3)–(9), we can express da_a, dl_a, da_z, dl_z, $d\alpha$, $d\beta$, and $d\phi_i$ as functions of f_1 and f_2.

The unit cell lengths can be expressed as

$$u_a = \frac{a_a}{2} + \frac{b_a}{2} + n\left(\frac{b_a}{2} + \frac{c_a}{2}\right) - a_z\cos\alpha$$

$$= a_a - b_z\cos\beta - \sum_{k=1}^{n}\left((b_z + c_z)\cos(\beta + \sum_{i=1}^{k}\phi_i)\right) \tag{10}$$

$$u_z = 2a_z\sin\alpha + b_z\sin\beta + \sum_{k=1}^{n}\left((b_z + c_z)\sin(\beta + \sum_{i=1}^{k}\phi_i)\right) \tag{11}$$

Equation (10) shows that u_a can be expressed in two formats. To ensure the geometric continuity, the variances of u_a obtained from the two expressions should be equal to each other, which indeed leads to a geometric compatible equation that gives the relation between f_1 and f_2.

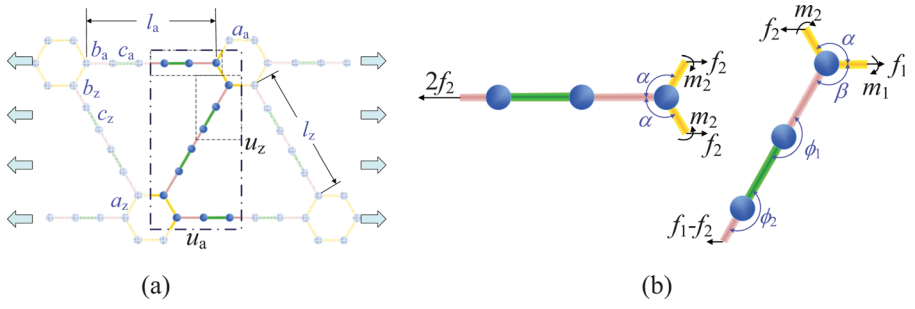

Fig. 2 (*a*) Graphene-*n* (*n* = 2) subject to tension. The dashed-dotted box indicates the unit cell (with lengths of u_a and u_z), while the dashed box marks are the representative local structures used in the present analytical model. (*b*) Force equilibrium of local structures.

$$f_1 = \gamma f_2 \tag{12}$$

in which

$$\gamma = \left(\frac{1}{4K_a} + \frac{5}{4K_n} + \frac{3(\lambda_2 C_{aa} - \lambda_1 C_{ab})r_0^2}{8(2C_{aa} + C_{ab})C_{ab}} + \frac{3\lambda_3 r_0^2}{8C_{bc}}\right) \Big/ \left(\frac{1}{2K_a} + \frac{1}{4K_n} + \frac{3(\lambda_2 C_{aa} - \lambda_1 C_{ab})r_0^2}{8(2C_{aa} + C_{ab})C_{ab}} + \frac{3\lambda_3 r_0^2}{8C_{bc}}\right)$$

with $\lambda_1 = \xi_a(\xi_b + n(\xi_b + \xi_c))$, $\lambda_2 = (\xi_b + n(\xi_b + \xi_c))^2$, $\lambda_3 = (\xi_b + \xi_c)\{[(n(n+1)(4n-1)/12)(\xi_b + \xi_c)] - [((2n+1) - (-1)^n/8)(\xi_b - \xi_c)]\}$, $\xi_a = a/r_0$, $\xi_b = b/r_0$, and $\xi_c = c/r_0$, where r_0 is the reference aromatic bond length in graphene.

Now, we are ready to write the expressions for the strains along the armchair and zigzag directions.

$$\varepsilon_a = \frac{du_a}{u_a} = \frac{f_2}{\eta a}\left(\frac{2\gamma + 1}{4K_a} + \frac{1}{K_n} + \frac{3(\gamma - 1)\lambda_1 r_0^2}{8(2C_{aa} + C_{ab})}\right) \tag{13}$$

$$\varepsilon_z = \frac{du_z}{u_z} = \frac{f_2}{\eta a}\left(\frac{1}{2K_a} + \frac{\gamma - 1}{4K_n} - \frac{(\gamma - 1)(2\lambda_1 + \lambda_2)r_0^2}{8(2C_{aa} + C_{ab})} - \frac{(\gamma - 1)\lambda_3 r_0^2}{8C_{bc}}\right) \tag{14}$$

where $\eta = \xi_a + [(n+1)/2]\xi_b + (n/2)\xi_c$.

The in-plane stiffness Y_S and Poisson's ratio ν can then be obtained as

$$Y_S = \frac{f_1 + f_2}{\sqrt{3}\eta a \varepsilon_a} = \frac{\gamma + 1}{\sqrt{3}} \Big/ \left(\frac{3(\gamma - 1)\lambda_1 r_0^2}{8(2C_{aa} + C_{ab})} + \frac{2\gamma + 1}{4K_a} + \frac{1}{K_n}\right) \tag{15}$$

$$\nu = -\frac{\varepsilon_z}{\varepsilon_a} = \left(\frac{(\gamma - 1)(2\lambda_1 + \lambda_2)r_0^2}{8(2C_{aa} + C_{ab})} + \frac{(\gamma - 1)\lambda_3 r_0^2}{8C_{bc}} - \frac{1}{2K_a} - \frac{\gamma - 1}{4K_n}\right) \Big/ \left(\frac{3(\gamma - 1)\lambda_1 r_0^2}{8(2C_{aa} + C_{ab})} + \frac{2\gamma + 1}{4K_a} + \frac{1}{K_n}\right) \tag{16}$$

Owing to the six-fold rotational symmetry of the lattice, the in-plane elastic properties of graphyne-n should be isotropic at infinitesimal strains. Equations (15) and (16) are indeed the expressions for the in-plane stiffness and Poisson's ratio of graphyne-n along arbitrary directions, even though they are obtained in the armchair direction. According to the isotropic elastic theory, the in-plane shear stiffness of graphyne-n can be expressed as

$$G_S = \frac{Y_S}{2(1 + \nu)} = \frac{\gamma + 1}{\sqrt{3}} \Big/ \left(\frac{(\gamma - 1)(2\lambda_1 + \lambda_2)r_0^2}{8(2C_{aa} + C_{ab})} + \frac{(\gamma - 1)\lambda_3 r_0^2}{8C_{bc}} - \frac{1}{2K_a} - \frac{\gamma - 1}{4K_n}\right) \tag{17}$$

For graphene, we have $n = 0$, $\gamma = 2$, $\lambda_1 = \lambda_2 = 1$, $\lambda_3 = 0$, $\eta = 3/2$, $K_a = K_0 = K$, and $C_{aa} = C_{ab} = C$. Equations (15)–(17) are thus reduced to

$$Y_S = \frac{8\sqrt{3}KC}{Kr_0^2 + 18C} \tag{18}$$

$$\nu = \frac{Kr_0^2 - 6C}{Kr_0^2 + 18C} \tag{19}$$

$$G_S = \frac{2\sqrt{3}KC}{Kr_0^2 + 6C} \tag{20}$$

which are identical to those obtained in the previous works [24,27].

Once the molecular parameters of graphene-n are determined, the in-plane stiffness, Poisson's ratio, and shear stiffness can be predicted using Eqs. (15)–(17). To show the applicability of these equations, we simply take $r_0 = 0.142$ nm, $\xi_a \approx \xi_b \approx 1$, $\xi_c \approx 0.85$ [6,9,11,16] and $K_a = 742$ nN/nm, $C_{aa} \approx C_{ab} = 1.42$ nN/nm [24]. Based on these values and Eqs. (15) and (16), taking $Y_S = 180$ N/m and $\nu = 0.19$ for graphyne [9] from MD simulations, we can obtain $K_n = 79.4\,\text{nN}/l = 559/(1.85n + 1)$ nN/nm, and $C_{bc} = 0.423$ nN/nm. We note that the obtained K_n and C_{bc} are in reasonable agreement in magnitude with existing numerical results. For example, MD simulations and first-principle calculations suggested that $K_n = 32.3$ [29], 159 [30], and 147 nN/l [31]; and $C_{bc} = 0.258$–0.384 [29], 0.109 [30], and 0.040 nN/nm [31].

Figures 3(*a*) and 3(*b*) depict the in-plane stiffness, shear stiffness, and Poisson's ratio of graphyne-n against the number of acetylenic linkages predicted by Eqs. (15)–(17). It is clearly seen that the in-plane stiffness of graphyne-n decreases with increasing acetylenic linkage number, and is in excellent agreement with the existing numerical results [7,10,13]. For instance, Yang and Xu [10] showed that with increasing acetylenic linkage number n from 1 to 5, the in-plane stiffness of graphyne-n degrades from 150 to 50 N/m with almost 67% reduction. This decreasing trend has been confirmed by Yue et al. [13] in their first-principle

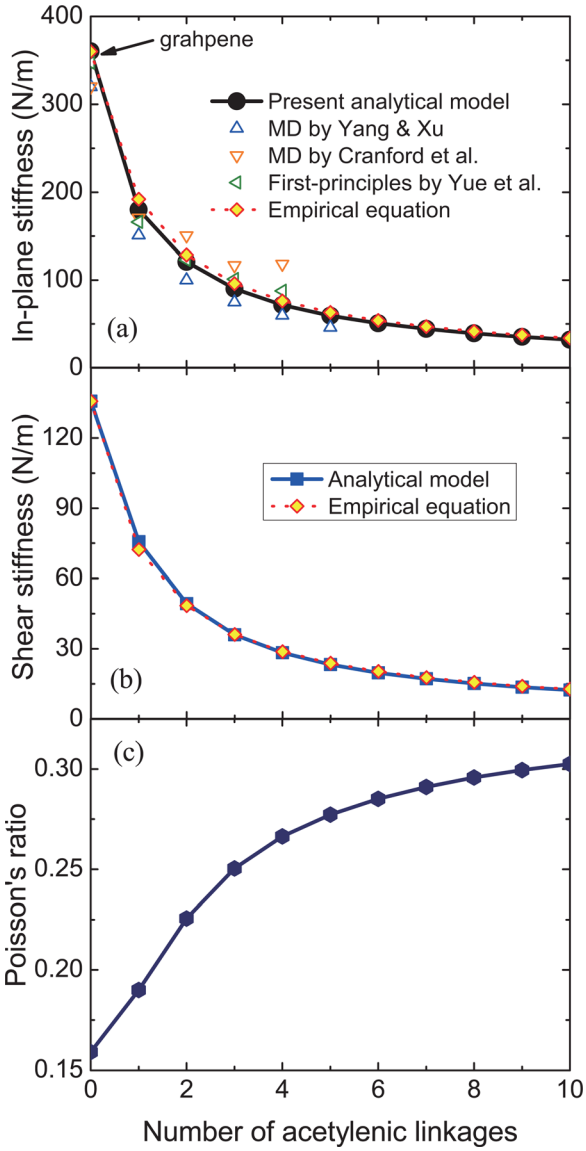

Fig. 3 (*a*) In-plane stiffness, (*b*) shear stiffness, and (*c*) Poisson's ratio of graphene-*n* as functions of the number of acetylenic linkages

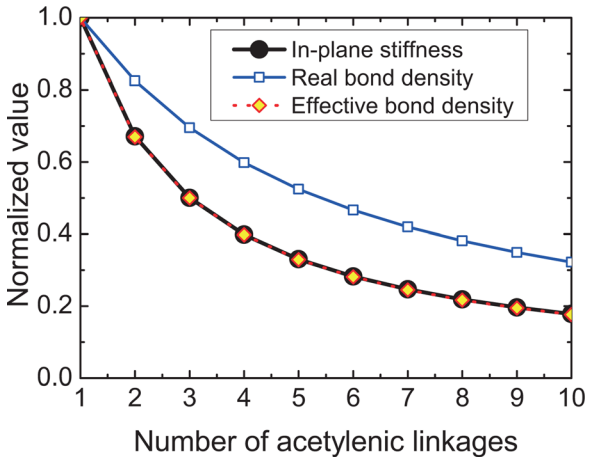

Fig. 4 Dependence of the normalized in-plane stiffness, real bond density, and effective bond density on the number of acetylenic linkages

calculations. Cranford et al. [7] further showed via a spring-network model that the in-plane stiffness of graphyne-*n* is approximately an inverse function of the number of acetylenic linkages. The shear stiffness too decreases with the number of acetylenic linkages, e.g., from 75.6 to 12.3 nN/nm with *n* from 1 to 10. The reduction in the in-plane stiffness and shear stiffness is attributed to the smaller atom/bond density, as will be shown next. In contrast to the in-plane stiffness, Poisson's ratio increases from 0.19 to 0.30 as the number of acetylenic linkages increases from 1 to 10, as shown in Fig. 3(*c*). This is because a longer acetylenic chain has a lower bending resistance which leads to a larger lateral deflection and thus to a higher Poisson's ratio.

At relatively large strains, the mechanical properties of graphyne-*n* along different directions may be different [6–13]. This is a consequence of the strain-induced anisotropy as found in carbon nanotubes and graphene [26,28]. It is noted that the present formulae are based solely on a static structural analysis, and the predictions are typically limited to idealized crystalline orientations when the deformations are restricted to in-plane. This is applicable to the mechanical properties of graphynes at an extremely low temperature or adhered to a substrate. For free-standing graphynes at relatively high temperatures, due to the out-of-plane rippling and deformation, it is unlikely the predicted Poisson's ratio would be observed. Further studies are needed.

3 Scaling Law

As the number of acetylenic linkages increases, the bond density in graphynes decreases. This is the main reason for the acetylenic linkage number dependent mechanical properties of graphyne-*n*. In this section, we will establish a scaling law for the in-plane stiffness of graphyne-*n* based on the bond density analysis.

The number of bonds per area, i.e., the bond density, in graphyne-*n* can be directly calculated by

$$\rho = \frac{4n+6}{\sqrt{3}(\eta+1/2)\eta r_0^2} \tag{21}$$

which is a decreasing function of the number of acetylenic linkages. As shown in Fig. 4, although the in-plane stiffness exhibits a decreasing trend as the bond density, the dependence of the in-plane stiffness on the number of acetylenic linkages is clearly different from that of the bond density.

We notice that $\gamma\ (=f_1/f_2)$ is close to 1 for graphyne-*n* (2 for graphene, 1.12 for $n=1$, decreasing with *n*). This means that the acetylenic chains along the zigzag direction have negligible contribution to the in-plane stiffness along the armchair direction, implying that the effective bond number for in-plane stiffness should be less than the real bond number. By taking an effective bond number equal to 1 (which can ensure consistency for graphene) for the acetylenic chain in the zigzag direction and a further simplification with $\xi_a \approx \xi_b \approx \xi_c \approx 1$, we have an effective bond density of graphyne-*n* as

$$\bar{\rho} = \frac{2n+6}{\sqrt{3}(n+2)(n+3/2)r_0^2} \tag{22}$$

It is surprising to see from Fig. 4 that the dependence of the effective bond density on the number of acetylenic linkages perfectly matches that of the in-plane stiffness. As a result, we can directly have an empirical equation for the in-plane stiffness of graphyne-*n*

$$Y_S = \frac{n+3}{(n+2)(n+3/2)} Y_S^{ge} \tag{23}$$

where Y_S^{ge} is the in-plane stiffness of graphene. As seen in Fig. 3(*a*), this empirical equation gives excellent predictions for the in-plane stiffness of graphyne-*n*, which confirms that the reduction of the in-plane stiffness of graphyne-*n* is a direct result of the reduction of the effective bond density (rather than the real bond density).

For the in-plane shear stiffness, similar to Eq. (23), we have

$$G_S = \frac{n+3}{(n+2)(n+3/2)} G_S^{ge} \tag{24}$$

where G_S^{ge} is the shear stiffness of graphene. Again, perfect agreement is found between the predictions from empirical equation (24) and analytical equation (17), as shown in Fig. 3(*b*).

Owing to the physical basis of bond density analysis, it is expected that some other mechanical properties such as tensile strength of graphyne-*n* would obey the same scaling law as the in-plane stiffness. For example, Cranford et al. [7] showed via a spring-network model that the in-plane stiffness and tensile strength are both inversely dependent on the number of acetylenic linkages of graphyne-*n* (which is consistent with the present scaling law for large *n*). The scaling law we obtained here for in-plane stiffness may thus have implications for other mechanical properties of graphyne-*n* and other types of graphynes.

4 Conclusions

In summary, based on a molecular mechanics approach, we have developed an analytical model to obtain closed-form expressions for mechanical properties of graphyne-*n*. These expressions are capable of linking macroscopic properties of graphyne-*n* to its atomic structure in a direct manner. The predicted results from the present analytical model are in good agreement with the existing numerical results from MD simulations and first-principle calculations. Based on an effective bond density analysis, we establish a scaling law for the in-plane stiffness of graphyne-*n* which gives predictions in excellent agreement with the analytical expressions. It is worth noting that, although herein we focus on the graphyne-*n* structures, the model developed in this work can be easily extended to predict the mechanical properties of other types of graphynes with some further modifications. In this sense, our molecular mechanics model provides a helpful tool for a better understanding of the mechanical properties of all different graphynes, which is of significant importance for the development of graphynes-based nanomechanical devices.

Acknowledgment

The authors acknowledge the financial supports from the NSF of China (Grant Nos. 11425209 and 11172160) and Shanghai Pujiang Program (Grant No. 13PJD016).

References

[1] Hirsch, A., 2010, "The Era of Carbon Allotropes," Nat. Mater., **9**(11), pp. 868–871.

[2] Diederich, F., and Kivala, M., 2010, "All-Carbon Scaffolds by Rational Design," Adv. Mater., **22**(7), pp. 803–812.

[3] Enyashin, A. N., and Ivanovskii, A. L., 2011, "Graphene Allotropes," Phys. Status Solidi B, **248**(8), pp. 1879–1883.

[4] Baughman, R. H., Eckhardt, H., and Kertesz, M., 1987, "Structure-Property Predictions for New Planar Forms of Carbon: Layered Phases Containing sp^2 and sp Atoms," J. Chem. Phys., **87**(11), pp. 6687–6699.

[5] Brommer, D. B., and Buehler, M. J., 2013, "Failure of Graphdiyne: Structurally Directed Delocalized Crack Propagation," ASME J. Appl. Mech., **80**(4), p. 040908.

[6] Cranford, S. W., and Buehler, M. J., 2011, "Mechanical Properties of Graphyne," Carbon, **49**(13), pp. 4111–4121.

[7] Cranford, S. W., Brommer, D. B., and Buehler, M. J., 2012, "Extended Graphynes: Simple Scaling Laws for Stiffness, Strength and Fracture," Nanoscale, **4**(24), pp. 7797–7809.

[8] Zhang, Y. Y., Pei, Q. X., and Wang, C. M., 2012, "Mechanical Properties of Graphynes Under Tension: A Molecular Dynamics Study," Appl. Phys. Lett., **101**(8), p. 081909.

[9] Zhao, J., Wei, N., Fan, Z., Jiang, J.-W., and Rabczuk, T., 2013, "The Mechanical Properties of Three Types of Carbon Allotropes," Nanotechnology, **24**(9), p. 095702.

[10] Yang, Y., and Xu, X., 2012, "Mechanical Properties of Graphyne and Its Family—A Molecular Dynamics Investigation," Comput. Mater. Sci., **61**, pp. 83–88.

[11] Peng, Q., Ji, W., and De, S., 2012, "Mechanical Properties of Graphyne Monolayers: A First-Principles Study," Phys. Chem. Chem. Phys., **14**(38), pp. 13385–13391.

[12] Wang, G., Si, M., Kumar, A., and Pandey, R., 2014, "Strain Engineering of Dirac Cones in Graphyne," Appl. Phys. Lett., **104**(21), p. 213107.

[13] Yue, Q., Chang, S., Kang, J., Qin, S., and Li, J., 2013, "Mechanical and Electronic Properties of Graphyne and Its Family Under Elastic Strain: Theoretical Predictions," J. Phys. Chem. C, **117**(28), pp. 14804–14811.

[14] Ducéré, J.-M., Lepetit, C., and Chauvin, R., 2013, "Carbo-Graphite: Structural, Mechanical, and Electronic Properties," J. Phys. Chem. C, **117**(42), pp. 21671–21681.

[15] Pan, L. D., Zhang, L. Z., Song, B. Q., Du, S. X., and Gao, H.-J., 2011, "Graphyne- and Graphdiyne-Based Nanoribbons: Density Functional Theory Calculations of Electronic Structures," Appl. Phys. Lett., **98**(17), p. 173102.

[16] Zhou, J., Lv, K., Wang, Q., Chen, X. S., Sun, Q., and Jena, P., 2011, "Electronic Structures and Bonding of Graphyne Sheet and Its BN Analog," J. Chem. Phys., **134**(17), p. 174701.

[17] Malko, D., Neiss, C., Viñes, F., and Görling, A., 2012, "Competition for Graphene: Graphynes With Direction-Dependent Dirac Cones," Phys. Rev. Lett., **108**(8), p. 086804.

[18] Kim, B. G., and Choi, H. J., 2012, "Graphyne: Hexagonal Network of Carbon With Versatile Dirac Cones," Phys. Rev. B, **86**(11), p. 115435.

[19] Sevinçli, H., and Sevik, C., 2014, "Electronic, Phononic, and Thermoelectric Properties of Graphyne Sheets," Appl. Phys. Lett., **105**(22), p. 223108.

[20] Li, Y., Xu, L., Liu, H., and Li, Y., 2014, "Graphdiyne and Graphyne: From Theoretical Predictions to Practical Construction," Chem. Soc. Rev., **43**(8), pp. 2572–2586.

[21] Sun, C., Liu, Y., Xu, J., Chi, B., Bai, C., Liu, Y., Li, S., Zhao, X., and Li, X., 2015, "Density Functional Study of α-Graphyne Derivatives: Energetic Stability, Atomic and Electronic Structure," Phys. E, **70**, pp. 190–197.

[22] Xue, M., Qiu, H., and Guo, W., 2013, "Exceptionally Fast Water Desalination at Complete Salt Rejection by Pristine Graphyne Monolayers," Nanotechnology, **24**(50), p. 505720.

[23] Jang, B., Koo, J., Park, M., Lee, H., Nam, J., Kwon, Y., and Lee, H., 2013, "Graphdiyne as a High-Capacity Lithium Ion Battery Anode Material," Appl. Phys. Lett., **103**(26), p. 263904.

[24] Chang, T., and Gao, H., 2003, "Size-Dependent Elastic Properties of a Single-Walled Carbon Nanotube Via a Molecular Mechanics Model," J. Mech. Phys. Solids, **51**(6), pp. 1059–1074.

[25] Chang, T., Geng, J., and Guo, X., 2005, "Chirality- and Size-Dependent Elastic Properties of Single-Walled Carbon Nanotubes," Appl. Phys. Lett., **87**(25), p. 251929.

[26] Geng, J., and Chang, T., 2006, "Nonlinear Stick-Spiral Model for Predicting Mechanical Behavior of Single-Walled Carbon Nanotubes," Phys. Rev. B, **74**(24), p. 245428.

[27] Chang, T., 2010, "A Molecular Based Anisotropic Shell Model for Single-Walled Carbon Nanotubes," J. Mech. Phys. Solids, **58**(9), pp. 1422–1433.

[28] Ma, T., Li, B., and Chang, T., 2011, "Chirality- and Curvature-Dependent Bending Stiffness of Single Layer Graphene," Appl. Phys. Lett., **99**(20), p. 201901.

[29] Nair, A. K., Cranford, S. W., and Buehler, M. J., 2011, "The Minimal Nanowire: Mechanical Properties of Carbyne," Europhys. Lett., **95**(1), p. 16002.

[30] Liu, M., Artyukhov, V. I., Lee, H., Xu, F., and Yakobson, B. I., 2013, "Carbyne From First Principles: Chain of C Atoms, a Nanorod or a Nanorope," ACS Nano, **7**(11), pp. 10075–10082.

[31] Ashley, J. K., Neta Aditya Reddy, Y., and Steven, W. C., 2014, "Confinement and Controlling the Effective Compressive Stiffness of Carbyne," Nanotechnology, **25**(33), p. 335709.

[32] Yuan, Q., and Ding, F., 2014, "Formation of Carbyne and Graphyne on Transition Metal Surfaces," Nanoscale, **6**(21), pp. 12727–12731.